



HAL
open science

Search for Scalar Leptons in e^+e^- collisions at $\sqrt{s}=189$ GeV

M. Acciarri, P. Achard, O. Adriani, M. Aguilar-Benitez, J. Alcaraz, G. Alemanni, J. Allaby, A. Aloisio, M G. Alviggi, G. Ambrosi, et al.

► **To cite this version:**

M. Acciarri, P. Achard, O. Adriani, M. Aguilar-Benitez, J. Alcaraz, et al.. Search for Scalar Leptons in e^+e^- collisions at $\sqrt{s}=189$ GeV. Physics Letters B, 1999, 471, pp.280-292. 10.1016/S0370-2693(99)01314-3. in2p3-00003720

HAL Id: in2p3-00003720

<https://hal.in2p3.fr/in2p3-00003720>

Submitted on 18 Jan 2000

HAL is a multi-disciplinary open access archive for the deposit and dissemination of scientific research documents, whether they are published or not. The documents may come from teaching and research institutions in France or abroad, or from public or private research centers.

L'archive ouverte pluridisciplinaire **HAL**, est destinée au dépôt et à la diffusion de documents scientifiques de niveau recherche, publiés ou non, émanant des établissements d'enseignement et de recherche français ou étrangers, des laboratoires publics ou privés.

**Search for Scalar Leptons in e^+e^- collisions
at $\sqrt{s} = 189$ GeV**

The L3 collaboration

Abstract

We report the result of a search for scalar leptons in e^+e^- collisions at 189 GeV centre-of-mass energy at LEP. No evidence for such particles is found in a data sample of 176 pb^{-1} . Improved upper limits are set on the production cross sections for these new particles. New exclusion contours in the parameter space of the Minimal Supersymmetric Standard Model are derived, as well as new lower limits on the masses of these supersymmetric particles. Under the assumptions of common gaugino and scalar masses at the GUT scale, we set an absolute lower limit on the mass of the lightest scalar electron of 65.5 GeV.

Submitted to *Phys. Lett. B*

1 Introduction

One of the main goals of the LEP experiments is to search for new particles predicted by theories beyond the Standard Model. In this letter we report on searches for unstable scalar leptons. These particles are predicted by supersymmetric theories (SUSY) [1]. In SUSY theories with minimal particle content (MSSM) [2], in addition to the ordinary particles, there is a supersymmetric spectrum of particles with spins which differ by one half with respect to their Standard Model partners.

Scalar leptons ($\tilde{\ell}_R^\pm$ and $\tilde{\ell}_L^\pm$) are the supersymmetric partners of the right- and left-handed leptons. Pair production takes place through s -channel γ/Z exchange. For scalar electrons the production cross section is enhanced by t -channel exchange of a neutralino.

Short-lived supersymmetric particles are expected in R-parity conserving SUSY models. The R-parity is a quantum number which distinguishes ordinary particles from supersymmetric particles. If R-parity is conserved supersymmetric particles are pair-produced and the lightest supersymmetric particle, the lightest neutralino $\tilde{\chi}_1^0$, is stable. The neutralino is weakly-interacting and escapes detection. In this letter we assume R-parity conservation, which implies that the decay chain of supersymmetric particles always contains, besides standard particles, two invisible neutralinos causing the missing energy signature.

The scalar lepton decays into its partner lepton mainly via $\tilde{\ell}^\pm \rightarrow \tilde{\chi}_1^0 \ell^\pm$, but also via the cascade decay, such as $\tilde{\ell}^\pm \rightarrow \tilde{\chi}_2^0 \ell^\pm \rightarrow \tilde{\chi}_1^0 Z^* \ell^\pm$, which may dominate in some regions of the parameter space of the MSSM.

Previous limits on scalar leptons have been obtained at lower energies by L3 [3–5] and other LEP experiments [6]. Results presented in this paper are organised as follows: Data sample and event simulation are presented in Section 2; Experimental signatures and event selections are discussed in Section 3; In Section 4 experimental results are summarised and in Section 5 model independent limits are presented on production cross sections. In Section 6, our experimental results are interpreted in the framework of the constrained MSSM, and in the minimal supergravity model. In these models, lower limits on the masses of supersymmetric particles are obtained. For these limits present experimental results are combined with those obtained previously by L3 at the Z peak [7] and at energies up to 183 GeV [3–5].

2 Data Sample and Simulation

We present the analysis of data collected with the L3 detector [8] in 1998, corresponding to an integrated luminosity of 176.3 pb^{-1} at an average centre-of-mass energy, \sqrt{s} , of 188.6 GeV, denoted hereafter as $\sqrt{s} = 189 \text{ GeV}$.

Standard Model reactions are simulated with the following Monte Carlo generators: PYTHIA [9] for $e^+e^- \rightarrow q\bar{q}$, $e^+e^- \rightarrow Ze^+e^-$ and $e^+e^- \rightarrow \gamma/Z\gamma/Z$; EXCALIBUR [10] for $e^+e^- \rightarrow W^\pm e^\mp \nu$; KORALZ [11] for $e^+e^- \rightarrow \mu^+\mu^-$ and $e^+e^- \rightarrow \tau^+\tau^-$; BHWIDE [12] for $e^+e^- \rightarrow e^+e^-$; KORALW [13] for $e^+e^- \rightarrow W^+W^-$; two-photon interaction processes have been simulated using DIAG36 [14] ($e^+e^- \rightarrow e^+e^-\ell^+\ell^-$) and PHOJET [15] ($e^+e^- \rightarrow e^+e^-$ hadrons), requiring at least 3 GeV for the invariant mass of the two-photon system. The number of simulated events for each background process is equivalent to more than 100 times the statistics of the collected data sample except for two-photon interactions for which it is more than two times the data statistics.

Signal events are generated with the Monte Carlo program SUSYGEN [16], for masses of SUSY particles (M_{SUSY}) ranging from 45 GeV up to the kinematic limit, and for ΔM values ($\Delta M = M_{\text{SUSY}} - M_{\tilde{\chi}_1^0}$) between 3 GeV and $M_{\text{SUSY}} - 1 \text{ GeV}$.

The detector response is simulated using the `GEANT` package [17]. It takes into account effects of energy loss, multiple scattering and showering in the detector materials and in the beam pipe. Hadronic interactions are simulated with the `GHEISHA` program [18]. Time dependent inefficiencies of the different subdetectors are also taken into account in the simulation procedure.

3 Analysis Procedure

3.1 Signal topologies and optimisation procedure

Besides the main characteristic of missing transverse momentum, supersymmetric particle signals can be further specified according to the number of leptons or the multiplicity of hadronic jets in the final state.

For scalar leptons, signatures are simple since most of the time the final state is given by two acoplanar leptons of the same generation. To account for the three lepton types three different selections are performed. While for scalar electrons and muons, two identified leptons are required in the event, scalar taus are selected as low multiplicity events with two narrow jets.

A new analysis searching for a single electron is also presented for the first time. This search accounts for $e^+e^- \rightarrow \tilde{e}_R\tilde{e}_L$ production when the \tilde{e}_R is almost mass degenerate with the $\tilde{\chi}_1^0$, since the \tilde{e}_L is heavier than the \tilde{e}_R . Thus the visible electron comes from the decay of $\tilde{e}_L \rightarrow \tilde{\chi}_1^0 e$, while the decay of \tilde{e}_R can be invisible for $\Delta M \sim 0$.

The ΔM dependence of the signal and background events is taken into account with different optimisations for each selection. For scalar electron and scalar muon analyses, three selections are performed: for the low ΔM range at 3 – 5 GeV, the medium ΔM range at 10 – 40 GeV and the high ΔM range at 60 – 90 GeV. For the scalar tau analysis, four selections are optimised for different ΔM ranges: 3 – 7 GeV, 7 – 15 GeV, 15 – 30 GeV, above 30 GeV.

The cut values of each selection are *a priori* optimised using Monte Carlo signal and background events. The optimisation procedure varies all cuts simultaneously to maximise the signal efficiency and the background rejection. In fact, we minimise the average limit (κ^{-1}), for infinite number of experiments, assuming only background contribution. This is expressed mathematically by the following formula:

$$\kappa = \epsilon / \sum_{n=0}^{\infty} k(b)_n P(b, n) \quad (1)$$

where $k(b)_n$ is the 95% confidence level Bayesian upper limit, $P(b, n)$ is the Poisson distribution for n events with an expected background of b events, and ϵ is the signal efficiency.

3.2 Event selection

Lepton and photon identification, and isolation criteria in hadronic events are unchanged compared to our previous analysis at $\sqrt{s} = 183$ GeV [4]. The Durham algorithm [19] is used for the clustering of hadronic jets.

Events are first selected by requiring at least 3 GeV of visible energy and 3 GeV of transverse momentum. Beam-gas events are rejected by requiring the visible energy in a cone of 30° around the beam pipe to be less than 90% of the total, and the missing momentum vector to be at least 10° away from the beam pipe. Tagged two-photon interactions are rejected by

requiring the sum of the energies measured in the lead-scintillator ring calorimeter and in the luminosity monitors [8] to be less than 10 GeV. These two detectors cover the polar angle range $1.5^\circ < \theta < 9^\circ$ on both sides of the interaction point.

Given the low multiplicity of the signal, events are rejected if the number of tracks is larger than 6 or if the number of calorimetric clusters (N_{cl}) is larger than 15. We then require two or three identified leptons and photons. The following quantities are defined: the energy depositions (E_{25}^\perp and E_{25}) within $\pm 25^\circ$ around the missing energy direction in the R- ϕ plane or in space respectively, and the energy deposition in a 60° half opening angle cone around the vector opposite to the sum of the two jet directions in space (E_{60}^b). We also apply cuts on the lepton energy (E_{lep}), on the total transverse momentum of the leptons (p_\perp), on their maximum acollinearity and acoplanarity, on the polar angle of the missing energy vector (θ_{miss}) and on the variable E_{TTL} . The latter is defined as the absolute value of the projection of the total momentum of the two highest energy leptons onto the direction perpendicular to the leptonic thrust computed in the R- ϕ plane.

The scalar taus are selected as low multiplicity events with acoplanar jets. Upper cuts on the jet width y_\perp , defined as the ratio between the sum of particle momenta transverse to the jet direction and the jet energy, are also applied. Distributions of the normalised transverse missing momentum p_\perp/E_{vis} are shown in Figure 1 for data, signal and background Monte Carlo events, at the preselection level.

The cut values optimised at $\sqrt{s} = 189$ GeV for the scalar lepton searches are quoted in Table 1 for the different ΔM ranges.

The single electron analysis makes use of very simple requirements aimed at a reliable identification of the electron and a nearly empty detector elsewhere. If two tracks are detected, their acoplanarity must be between 10° and 160° . The electron energy has to be less than 65 GeV to reject photon conversion from $e^+e^- \rightarrow \nu\bar{\nu}\gamma$, when the two tracks are not resolved. The energy of a second electron should be less than 4 GeV, and its acoplanarity with respect to the highest energy electron must be at least 20° . If only one electron is detected, the missing transverse momentum is required to be at least 6 GeV. If a second electron of at least 100 MeV is detected, the missing transverse momentum must be greater than 10 GeV.

4 Results

The results obtained at $\sqrt{s} = 189$ GeV for the ten scalar lepton selections are shown in Table 2. In this table, the results for the two lowest ΔM selections for scalar taus are shown together. A good agreement between the expected background from Standard Model processes and the selected data is observed.

The ten scalar lepton analyses performed at $\sqrt{s} = 189$ GeV select 21, 19 and 56 candidates in the scalar electron, muon and tau channels, respectively. Those observations are in good agreement with the background expectation of 23.0, 21.0 and 51.6 events, respectively.

All the scalar lepton selections are parametrised as a function of a single parameter, ξ , in the following manner: given a lower edge, X_{loose}^i , and an upper edge, X_{tight}^i , for the cut on variable i , the parameter ξ is equal to 0 when this cut is at the lower edge (many background events satisfy the selection) and to 100 when it is at the upper edge (no or few background events pass the selection). All cuts ($i = 1, \dots, N$) are related to the parameter ξ as follows:

$$X_{cut}^i = X_{loose}^i + (X_{tight}^i - X_{loose}^i) \times \frac{\xi}{100}.$$

The parameter ξ is scanned around the optimal value ($\xi = 50$) to check the agreement between data and Monte Carlo at different background rejection stages. As illustrated in Figure 2 for electrons and muons, and for several ΔM ranges, the data and Monte Carlo simulations are in good agreement. The vertical arrows show the ξ value corresponding to the optimised cuts.

For intermediate ΔM values different from those chosen for optimisation, we choose the combination of selections among those previously defined, providing the highest sensitivity [4]. In this combination procedure, we take into account the overlap among the selections within the data and Monte Carlo samples.

The selection efficiencies at $\sqrt{s} = 189$ GeV for scalar lepton pair production, as well as the background expectations, are reported for different values of ΔM in Table 3. Efficiencies vary from 19% to 58% for scalar electrons and from 11% to 36% for scalar muons. In comparison, the scalar tau selection efficiencies are smaller, ranging from 1.4% to 30%.

With the single electron analysis, 13 events are selected in data and 14.0 are expected from Standard Model processes. The transverse momentum distributions for the selected data, signal and background Monte Carlo events are shown in Figure 3. Signal efficiencies vary from 4% at $m_{\tilde{e}_L} - m_{\tilde{\chi}_1^0} = 5$ GeV to 60% at $m_{\tilde{e}_L} - m_{\tilde{\chi}_1^0} = 50$ GeV, and they do not change for any values of $m_{\tilde{e}_R} - m_{\tilde{\chi}_1^0}$ smaller than 4 GeV.

Systematic errors on the signal efficiencies are evaluated as in Reference 3, and they are typically 5% relative, dominated by Monte Carlo statistics. These errors are taken into account following the procedure explained in Reference 20.

5 Model independent upper limits on production cross sections

No excess of events is observed and we set upper limits on scalar lepton production cross sections. Exclusion limits at 95% C.L. are derived taking into account background contributions.

To derive the new upper limits on the production cross sections, and for interpretations in the MSSM we combine the 1998 data sample collected at $\sqrt{s} = 189$ GeV with those collected at lower centre-of-mass energies.

Assuming a branching fraction for $\tilde{\ell}^\pm \rightarrow \tilde{\chi}_1^0 \ell^\pm$ of 100%, upper limits are set on pair production cross sections of scalar electrons, muons and taus in the plane $M_{\tilde{\chi}_1^0}$ versus $M_{\tilde{\ell}^\pm}$ as depicted in Figure 4. The efficiency for the selection of scalar electrons includes the t -channel contribution. For scalar electron and muon masses below 94 GeV, and ΔM sufficiently large, cross sections above 0.1 pb are excluded. Owing to the lower selection sensitivity, the corresponding upper limit for the scalar tau cross section is 0.3 pb.

6 Limits on scalar lepton masses in the MSSM

In the MSSM, with Grand Unification assumptions [21], the masses and couplings of the SUSY particles as well as their production cross sections, are entirely described [2] once five parameters are fixed: $\tan \beta$, the ratio of the vacuum expectation values of the two Higgs doublets, $M \equiv M_2$, the gaugino mass parameter, μ , the higgsino mixing parameter, m_0 , the common mass for scalar fermions at the GUT scale, and A , the trilinear coupling in the Higgs sector. We investigate

the following MSSM parameter space:

$$\begin{aligned} 1 \leq \tan\beta &\leq 60, & 0 \text{ GeV} \leq M_2 &\leq 2000 \text{ GeV}, \\ -2000 \text{ GeV} \leq \mu &\leq 2000 \text{ GeV}, & 0 \text{ GeV} \leq m_0 &\leq 500 \text{ GeV}. \end{aligned}$$

All the limits on the cross sections previously shown combined with the results obtained at lower centre-of-mass energies, and for the mSUGRA interpretation with the recent results of chargino and neutralino searches [22], can be translated into exclusion regions in the MSSM parameter space. To derive limits in the MSSM, we optimise the global selection for any different point in the parameter space. This is obtained, choosing every time the combination of selections providing the highest sensitivity, given the production cross sections and the decay branching fractions which are calculated with the generator **SUSYGEN**.

In general, the SUSY partners of the right-handed leptons ($\tilde{\ell}_R^\pm$) are expected to be lighter than their counterparts for left-handed leptons. Hence, we show in Figures 5a, 5b and 5c the exclusion contours in the $M_{\tilde{\chi}_1^0} - M_{\tilde{\ell}_R^\pm}$ plane considering only the reaction $e^+e^- \rightarrow \tilde{\ell}_R^\pm \tilde{\ell}_R^\mp$ and setting $\mu = -200 \text{ GeV}$ and $\tan\beta = \sqrt{2}$. These exclusions hold also for higher $\tan\beta$ and $|\mu|$ values. For smaller $|\mu|$ values, the t -channel contribution to the scalar electron cross section is reduced, thus reducing by a few GeV the limit on its mass shown in Figure 5a. The values of μ and $\tan\beta$ are also relevant for the calculation of the branching ratio for the decay $\tilde{\ell}^\pm \rightarrow \tilde{\chi}_2^0 \ell^\pm \rightarrow \tilde{\chi}_1^0 Z^* \ell^\pm$ in Figures 5a–c. To derive these exclusions, only the purely leptonic decay $\tilde{\ell}_R^\pm \rightarrow \ell^\pm \tilde{\chi}_1^0$ is considered, neglecting any additional efficiency from cascade decays.

Under these assumptions lower limits on scalar lepton masses are derived. From Figures 5a and 5b scalar electrons lighter than 85.5 GeV, for $\Delta M > 10 \text{ GeV}$, and scalar muons lighter than 78 GeV, for $\Delta M > 15 \text{ GeV}$, are excluded. Including also the contribution from the process $e^+e^- \rightarrow \tilde{e}_R \tilde{e}_L$ and using the single electron selection, the very small ΔM region for the \tilde{e}_R can be excluded at 95% C.L. up to $M_{\tilde{e}_R^\pm} = 69.6 \text{ GeV}$. This additional exclusion is shown as the dark area in Figure 5a. From Figure 5c we conclude that scalar taus lighter than 65 GeV, for $10 \text{ GeV} < \Delta M < 40 \text{ GeV}$, are excluded if there is no mixing.

Mass eigenstates of scalar leptons are in general a mixture of the weak eigenstates $\tilde{\ell}_R^\pm$ and $\tilde{\ell}_L^\pm$. The mixing between $\tilde{\ell}_R^\pm$ and $\tilde{\ell}_L^\pm$ is proportional to the mass of the partner lepton. Hence the mixing for scalar electrons and muons is always negligible while it can be sizable for scalar taus. The mixing is governed by the parameters A , μ and $\tan\beta$.

Scalar tau mass eigenstates are given by $\tilde{\tau}_{1,2} = \tilde{\tau}_{L,R} \cos\theta_{LR} \pm \tilde{\tau}_{R,L} \sin\theta_{LR}$, where θ_{LR} is the mixing angle. The production cross section for scalar taus can be parametrised as a function of the scalar tau mass and of the mixing angle [23]. At $\theta_{LR} \sim 52^\circ$ the scalar tau decouples from the Z and the cross section is minimal. It reaches the maximum at $\cos\theta_{LR}=1$ when the scalar tau is equivalent to the weak eigenstate $\tilde{\tau}_L^\pm$.

The exclusion contours in Figure 5d are obtained considering only the reaction $e^+e^- \rightarrow \tilde{\tau}_1^+ \tilde{\tau}_1^-$ and assuming 100% branching ratio for $\tilde{\tau}_1 \rightarrow \tau \tilde{\chi}_1^0$. The two contours correspond to the minimal and maximal cross sections. Under the most conservative assumption for the mixing, a scalar tau lighter than 60 GeV is excluded for ΔM values between 8 and 42 GeV. In case of $\cos\theta_{LR} = 1$ the mass limit reaches 71.5 GeV assuming ΔM greater than 12 GeV.

The limiting factor towards an absolute limit on the scalar electron mass was the lack of detection efficiency for very small ΔM values. This can be overcome in the constrained MSSM by taking profit of the $e^+e^- \rightarrow \tilde{e}_R \tilde{e}_L$ process. The searches for acoplanar electrons at centre-of-mass energies between 130 GeV and 189 GeV, and single electrons at $\sqrt{s} = 189 \text{ GeV}$ have been combined to derive a lower limit on $M_{\tilde{e}_R}$ as a function of $\tan\beta$ and for any value of m_0 , M_2 and μ as shown in Figure 6. The new lower limit for the lightest scalar electron independent

of the MSSM parameters, found at $\tan\beta = 1$, is:

$$M_{\tilde{e}_R} \geq 65.5 \text{ GeV}.$$

Assuming a common mass for the scalar leptons at the GUT scale, this limit holds also for the lightest scalar muon, $\tilde{\mu}_R$.

Mass limits on scalar electrons and muons can also be expressed in terms of the M_2 and m_0 parameters. This is shown in Figure 7 where exclusion domains in the $M_2 - m_0$ plane are determined in the minimal supergravity framework for $A_0 = 0$, $\tan\beta = 2$ and $\mu < 0$. The exclusion regions in Figure 7 are obtained by combining scalar electron and muon searches with chargino and neutralino searches [22]. The two contributions are well separated, as the contribution from scalar lepton searches is dominant for $m_0 \lesssim 70$ GeV while that from chargino and neutralino is dominant for $m_0 \gtrsim 70$ GeV.

Acknowledgments

We express our gratitude to the CERN accelerator divisions for the excellent performance of the LEP machine. We also acknowledge and appreciate the effort of the engineers, technicians and support staff who have participated in the construction and maintenance of this experiment.

References

- [1] Y.A. Golfand and E.P. Likhtman, Sov. Phys. JETP **13** (1971) 323;
D.V. Volkhov and V.P. Akulov, Phys. Lett. **B 46** (1973) 109;
J. Wess and B. Zumino, Nucl. Phys. **B 70** (1974) 39;
P. Fayet and S. Ferrara, Phys. Rep. **C 32** (1977) 249;
A. Salam and J. Strathdee, Fortschr. Phys. **26** (1978) 57.
- [2] H. P. Nilles, Phys. Rep. **110** (1984) 1;
H. E. Haber and G. L. Kane, Phys. Rep. **117** (1985) 75;
R. Barbieri, Nuovo Cimento **11** No. 4 (1988) 1.
- [3] L3 Collab., M. Acciarri *et al.*, Phys. Lett. **B 377** (1996) 289.
- [4] L3 Collab., M. Acciarri *et al.*, Eur. Phys. Journal **C 4** (1998) 207.
- [5] L3 Collab., M. Acciarri *et al.*, Phys. Lett. **B 456** (1999) 283.
- [6] ALEPH Collab., R. Barate *et al.*, Phys. Lett. **B 433** (1998) 176;
DELPHI Collab., P. Abreu *et al.*, Eur. Phys. Journal **C 6** (1999) 371;
OPAL Collab., G. Abbiendi *et al.*, CERN-EP-98-122, (1998).
- [7] L3 Collab., O. Adriani *et al.*, Phys. Rep. **236** (1993) 1;
L3 Collab., M. Acciarri *et al.*, Phys. Lett. **B 350** (1995) 109.
- [8] L3 Collab., B. Adeva *et al.*, Nucl. Instr. and Meth. **A 289** (1990) 35;
M. Chemarin *et al.*, Nucl. Instr. and Meth. **A 349** (1994) 345;
M. Acciarri *et al.*, Nucl. Instr. and Meth. **A 351** (1994) 300;
G. Basti *et al.*, Nucl. Instr. and Meth. **A 374** (1996) 293;
I.C. Brock *et al.*, Nucl. Instr. and Meth. **A 381** (1996) 236;
A. Adam *et al.*, Nucl. Instr. and Meth. **A 383** (1996) 342.
- [9] T. Sjöstrand, “PYTHIA 5.7 and JETSET 7.4 Physics and Manual”,
CERN–TH/7112/93 (1993), revised August 1995;
T. Sjöstrand, Comp. Phys. Comm. **82** (1994) 74.
- [10] EXCALIBUR version 1.11 is used.
F.A. Berends, R. Kleiss and R. Pittau, Nucl. Phys. **B 424** (1994) 308; Nucl. Phys. **B 426**
(1994) 344; Nucl. Phys. (Proc. Suppl.) **B 37** (1994) 163; Phys. Lett. **B 335** (1994) 490;
Comp. Phys. Comm. **83** (1994) 141.
- [11] KORALZ version 4.02 is used.
S. Jadach, B.F.L. Ward and Z. Wąs, Comp. Phys. Comm. **79** (1994) 503.
- [12] BHWIDE version 1.01 is used.
S. Jadach *et al.*, Phys. Lett. **B 390** (1997) 298.
- [13] KORALW version 1.33 is used.
M. Skrzypek *et al.*, Comp. Phys. Comm. **94** (1996) 216;
M. Skrzypek *et al.*, Phys. Lett. **B 372** (1996) 289.
- [14] F.A. Berends, P.H. Daverfeldt and R. Kleiss, Nucl. Phys. **B 253** (1985) 441.

- [15] PHOJET version 1.10 is used.
R. Engel, Z. Phys. **C 66** (1995) 203;
R. Engel and J. Ranft, Phys. Rev. **D 54** (1996) 4244.
- [16] SUSYGEN version 2.2 is used.
S. Katsanevas and P. Morawitz, Comp. Phys. Comm. **112** (1998) 227.
- [17] The L3 detector simulation is based on GEANT Version 3.15.
See R. Brun *et al.*, “GEANT 3”, CERN DD/EE/84-1 (Revised), September 1987.
- [18] H. Fesefeldt, RWTH Aachen Preprint PITHA 85/02 (1985).
- [19] S. Catani *et al.*, Phys. Lett. **B 269** (1991) 432;
S. Bethke *et al.*, Nucl. Phys. **B 370** (1992) 310.
- [20] R.D. Cousins and V.L. Highland, Nucl. Inst. Meth. **A 320** (1992) 331.
- [21] See for instance:
L. Ibanez, Phys. Lett. **B 118** (1982) 73;
R. Barbieri, S. Farrara and C. Savoy, Phys. Lett. **B 119** (1982) 343.
- [22] L3 Collab., M. Acciarri *et al.*, *Search for charginos and Neutralinos in e^+e^- collisions at $\sqrt{s}=189$ GeV*, contributed paper n. 7-46 to *EPS-HEP99*, Tampere, July 1999, and also submitted to Phys. Lett.
- [23] A. Bartl *et al.*, Z. Phys. **C 73** (1997) 469.
- [24] D0 Collab., S. Abachi *et al.*, Proceedings of the 28th ICHEP, Warsaw, (1996);
D0 Collab., B. Abbott *et al.*, Proceedings of the XVIII Int. Symposium on Lepton Photon Interactions, Hamburg, (1997);
D0 Collab., B. Abbott *et al.*, FERMILAB-PUB-98/402-E, submitted to Phys. Rev. Lett.

The L3 Collaboration:

M. Acciarri,²⁶ P. Achard,¹⁹ O. Adriani,¹⁶ M. Aguilar-Benitez,²⁵ J. Alcaraz,²⁵ G. Alemani,²² J. Allaby,¹⁷ A. Aloisio,²⁸ M. G. Alvigi,²⁸ G. Ambrosi,¹⁹ H. Anderhub,⁴⁷ V. P. Andreev,^{6,36} T. Angelescu,¹² F. Anselmo,⁹ A. Arefiev,²⁷ T. Azemoon,³ T. Aziz,¹⁰ P. Bagnaia,³⁵ L. Baksay,⁴² A. Balandras,⁴ R. C. Ball,³ S. Banerjee,¹⁰ Sw. Banerjee,¹⁰ A. Barczyk,^{47,45} R. Barillere,¹⁷ L. Barone,³⁵ P. Bartalini,²² M. Basile,⁹ R. Battiston,³² A. Bay,²² F. Becattini,¹⁶ U. Becker,¹⁴ F. Behner,⁴⁷ L. Bellucci,¹⁶ J. Berdugo,²⁵ P. Berges,¹⁴ B. Bertucci,³² B. L. Betev,⁴⁷ S. Bhattacharya,¹⁰ M. Biasini,³² A. Biland,⁴⁷ J. J. Blaising,⁴ S. C. Blyth,³³ G. J. Bobbink,² A. Böhm,¹ L. Boldizsar,¹³ B. Borgia,³⁵ D. Bourilkov,⁴⁷ M. Bourquin,¹⁹ S. Braccini,¹⁹ J. G. Branson,³⁸ V. Brigljevic,⁴⁷ F. Brochu,⁴ A. Buffini,¹⁶ A. Buijs,⁴³ J. D. Burger,¹⁴ W. J. Burger,³² J. Busenitz,⁴² A. Button,³ X. D. Cai,¹⁴ M. Campanelli,⁴⁷ M. Capell,¹⁴ G. Cara Romeo,⁹ G. Carlino,²⁸ A. M. Cartacci,¹⁶ J. Casaus,²⁵ G. Castellini,¹⁶ F. Cavallari,³⁵ N. Cavallo,²⁸ C. Cecchi,¹⁹ M. Cerrada,²⁵ F. Cesaroni,²³ M. Chamizo,¹⁹ Y. H. Chang,⁴⁹ U. K. Chaturvedi,¹⁸ M. Chemarin,²⁴ A. Chen,⁴⁹ G. Chen,⁷ G. M. Chen,⁷ H. F. Chen,²⁰ H. S. Chen,⁷ X. Chereau,⁴ G. Chiefari,²⁸ L. Cifarelli,³⁷ F. Cindolo,⁹ C. Civinini,¹⁶ I. Clare,¹⁴ R. Clare,¹⁴ G. Coignet,⁴ A. P. Colijn,² N. Colino,²⁵ S. Costantini,⁸ F. Cotorobai,¹² B. Cozzoni,⁹ B. de la Cruz,²⁵ A. Csilling,¹³ S. Cucciarelli,³² T. S. Dai,¹⁴ J. A. van Dalen,³⁰ R. D'Alessandro,¹⁶ R. de Asmundis,²⁸ P. Déglon,¹⁹ A. Degré,⁴ K. Deiters,⁴⁵ D. della Volpe,²⁸ P. Denes,³⁴ F. DeNotaristefani,³⁵ A. De Salvo,⁴⁷ M. Diemoz,³⁵ D. van Dierendonck,² F. Di Lodovico,⁴⁷ C. Dionisi,³⁵ M. Dittmar,⁴⁷ A. Dominguez,³⁸ A. Doria,²⁸ M. T. Dova,^{18,†} D. Duchesneau,⁴ D. Dufournaud,⁴ P. Duinker,² I. Duran,³⁹ H. El Mamouni,²⁴ A. Engler,³³ F. J. Eppling,¹⁴ F. C. Erne,² P. Extermann,¹⁹ M. Fabre,⁴⁵ R. Faccini,³⁵ M. A. Falagan,²⁵ S. Falciano,^{35,17} A. Favara,¹⁷ J. Fay,²⁴ O. Fedin,³⁶ M. Felcini,⁴⁷ T. Ferguson,³³ F. Ferroni,³⁵ H. Fesefeldt,¹ E. Fiandrina,³² J. H. Field,¹⁹ F. Filthaut,¹⁷ P. H. Fisher,¹⁴ I. Fisk,³⁸ G. Forconi,¹⁴ L. Fredj,¹⁹ K. Freudenreich,⁴⁷ C. Furetta,²⁶ Yu. Galaktionov,^{27,14} S. N. Ganguli,¹⁰ P. Garcia-Abia,⁵ M. Gataullin,³¹ S. S. Gau,¹¹ S. Gentile,^{35,17} N. Gheordanescu,¹² S. Giagu,³⁵ Z. F. Gong,²⁰ G. Grenier,²⁴ O. Grimm,⁴⁷ M. W. Gruenewald,⁸ M. Guida,³⁷ R. van Gulik,² V. K. Gupta,³⁴ A. Gurtu,¹⁰ L. J. Gutay,⁴⁴ D. Haas,⁵ A. Hasan,²⁹ D. Hatzifotiadou,⁹ T. Hebbeker,⁸ A. Hervé,¹⁷ P. Hidas,¹³ J. Hirschfelder,³³ H. Hofer,⁴⁷ G. Holzner,⁴⁷ H. Hoorani,³³ S. R. Hou,⁴⁹ I. Iashvili,⁴⁶ B. N. Jin,⁷ L. W. Jones,³ P. de Jong,² I. Josa-Mutuberría,²⁵ R. A. Khan,¹⁸ D. Kamrad,⁴⁶ M. Kaur,^{18,◇} M. N. Kienzle-Focacci,¹⁹ D. Kim,³⁵ D. H. Kim,⁴¹ J. K. Kim,⁴¹ S. C. Kim,⁴¹ J. Kirkby,¹⁷ D. Kiss,¹³ W. Kittel,³⁰ A. Klimentov,^{14,27} A. C. König,³⁰ A. Kopp,⁴⁶ I. Korolko,²⁷ V. Koutsenko,^{14,27} M. Kräber,⁴⁷ R. W. Kraemer,³³ W. Krenz,¹ A. Kunin,^{14,27} P. Ladron de Guevara,²⁵ I. Laktineh,²⁴ G. Landi,¹⁶ K. Lassila-Perini,⁴⁷ P. Laurikainen,²¹ A. Lavorato,³⁷ M. Lebeau,¹⁷ A. Lebedev,¹⁴ P. Lebrun,²⁴ P. Lecomte,⁴⁷ P. Lecoq,¹⁷ P. Le Coultre,⁴⁷ H. J. Lee,⁸ J. M. Le Goff,¹⁷ R. Leiste,⁴⁶ E. Leonardi,³⁵ P. Levchenko,³⁶ C. Li,²⁰ C. H. Lin,⁴⁹ W. T. Lin,⁴⁹ F. L. Linde,² L. Lista,²⁸ Z. A. Liu,⁷ W. Lohmann,⁴⁶ E. Longo,³⁵ Y. S. Lu,⁷ K. Lübelmeyer,¹ C. Luci,^{17,35} D. Luckey,¹⁴ L. Lugnier,²⁴ L. Luminari,³⁵ W. Lustermaan,⁴⁷ W. G. Ma,²⁰ M. Maity,¹⁰ L. Malgeri,¹⁷ A. Malinin,^{27,17} C. Mañá,²⁵ D. Mangeol,³⁰ P. Marchesini,⁴⁷ G. Marian,¹⁵ J. P. Martin,²⁴ F. Marzano,³⁵ G. G. Massaro,² K. Mazumdar,¹⁰ R. R. McNeil,⁶ S. Mele,¹⁷ L. Merola,²⁸ M. Meschini,¹⁶ W. J. Metzger,³⁰ M. von der Mey,¹ A. Mihul,¹² H. Milcent,¹⁷ G. Mirabelli,³⁵ J. Mnich,¹⁷ G. B. Mohanty,¹⁰ P. Molnar,⁸ B. Monteleoni,^{16,†} T. Moulik,¹⁰ G. S. Muanza,²⁴ F. Muheim,¹⁹ A. J. M. Muijs,² M. Musy,³⁵ M. Napolitano,²⁸ F. Nessi-Tedaldi,⁴⁷ H. Newman,³¹ T. Niessen,¹ A. Nisati,³⁵ H. Nowak,⁴⁶ Y. D. Oh,⁴¹ G. Organtini,³⁵ R. Ostonen,²¹ C. Palomares,²⁵ D. Pandoulas,¹ S. Paoletti,^{35,17} P. Paolucci,²⁸ R. Paramatti,³⁵ H. K. Park,³³ I. H. Park,⁴¹ G. Pascale,³⁵ G. Passaleva,¹⁷ S. Patricelli,²⁸ T. Paul,¹¹ M. Pauluzzi,³² C. Paus,¹⁷ F. Pauss,⁴⁷ D. Peach,¹⁷ M. Pedace,³⁵ S. Pensotti,²⁶ D. Perret-Gallix,⁴ B. Petersen,³⁰ D. Piccolo,²⁸ F. Pierella,⁹ M. Pieri,¹⁶ P. A. Piroué,³⁴ E. Pistolesi,²⁶ V. Plyaskin,²⁷ M. Pohl,⁴⁷ V. Pojidaev,^{27,16} H. Postema,¹⁴ J. Pothier,¹⁷ N. Produit,¹⁹ D. O. Prokofiev,⁴⁴ D. Prokofiev,³⁶ J. Quartieri,³⁷ G. Rahal-Callot,^{47,17} M. A. Rahaman,¹⁰ P. Raics,¹⁵ N. Raja,¹⁰ R. Ramelli,⁴⁷ P. G. Rancoita,²⁶ G. Raven,³⁸ P. Razis,²⁹ D. Ren,⁴⁷ M. Rescigno,³⁵ S. Reucroft,¹¹ T. van Rhee,⁴³ S. Riemann,⁴⁶ K. Riles,³ A. Robohm,⁴⁷ J. Rodin,⁴² B. P. Roe,³ L. Romero,²⁵ A. Rosca,⁸ S. Rosier-Lees,⁴ J. A. Rubio,¹⁷ D. Ruschmeier,⁸ H. Rykaczewski,⁴⁷ S. Saremi,⁶ S. Sarkar,³⁵ J. Salicio,¹⁷ E. Sanchez,¹⁷ M. P. Sanders,³⁰ M. E. Sarakinos,²¹ C. Schäfer,¹ V. Schegelsky,³⁶ S. Schmidt-Kaerst,¹ D. Schmitz,¹ H. Schopper,⁴⁸ D. J. Schotanus,³⁰ G. Schwering,¹ C. Sciacca,²⁸ D. Sciarrino,¹⁹ A. Seganti,⁹ L. Servoli,³² S. Shevchenko,³¹ N. Shivarov,⁴⁰ V. Shoutko,²⁷ E. Shumilov,²⁷ A. Shvorob,³¹ T. Siedenburger,¹ D. Son,⁴¹ B. Smith,³³ P. Spillantini,¹⁶ M. Steuer,¹⁴ D. P. Stickland,³⁴ A. Stone,⁶ H. Stone,^{34,†} B. Stoyanov,⁴⁰ A. Straessner,¹ K. Sudhakar,¹⁰ G. Sultanov,¹⁸ L. Z. Sun,²⁰ H. Suter,⁴⁷ J. D. Swain,¹⁸ Z. Szillasi,^{42,¶} T. Sztaricskai,^{42,¶} X. W. Tang,⁷ L. Tauscher,⁵ L. Taylor,¹¹ C. Timmermans,³⁰ Samuel C. C. Ting,¹⁴ S. M. Ting,¹⁴ S. C. Tonwar,¹⁰ J. Tóth,¹³ C. Tully,³⁴ K. L. Tung,⁷ Y. Uchida,¹⁴ J. Ulbricht,⁴⁷ E. Valente,³⁵ G. Vesztegombi,¹³ I. Vetlitsky,²⁷ D. Vicinanza,³⁷ G. Viertel,⁴⁷ S. Villa,¹¹ M. Vivargent,⁴ S. Vlachos,⁵ I. Vodopianov,³⁶ H. Vogel,³³ H. Vogt,⁴⁶ I. Vorobiev,²⁷ A. A. Vorobyov,³⁶ A. Vorvolakos,²⁹ M. Wadhwa,⁵ W. Wallraff,¹ M. Wang,¹⁴ X. L. Wang,²⁰ Z. M. Wang,²⁰ A. Weber,¹ M. Weber,¹ P. Wienemann,¹ H. Wilkens,³⁰ S. X. Wu,¹⁴ S. Wynhoff,¹ L. Xia,³¹ Z. Z. Xu,²⁰ B. Z. Yang,²⁰ C. G. Yang,⁷ H. J. Yang,⁷ M. Yang,⁷ J. B. Ye,²⁰ S. C. Yeh,⁵⁰ An. Zalite,³⁶ Yu. Zalite,³⁶ Z. P. Zhang,²⁰ G. Y. Zhu,⁷ R. Y. Zhu,³¹ A. Zichichi,^{9,17,18} F. Ziegler,⁴⁶ G. Zilizi,^{42,¶} M. Zöller.¹

- 1 I. Physikalisches Institut, RWTH, D-52056 Aachen, FRG[§]
III. Physikalisches Institut, RWTH, D-52056 Aachen, FRG[§]
 - 2 National Institute for High Energy Physics, NIKHEF, and University of Amsterdam, NL-1009 DB Amsterdam, The Netherlands
 - 3 University of Michigan, Ann Arbor, MI 48109, USA
 - 4 Laboratoire d'Annecy-le-Vieux de Physique des Particules, LAPP, IN2P3-CNRS, BP 110, F-74941 Annecy-le-Vieux CEDEX, France
 - 5 Institute of Physics, University of Basel, CH-4056 Basel, Switzerland
 - 6 Louisiana State University, Baton Rouge, LA 70803, USA
 - 7 Institute of High Energy Physics, IHEP, 100039 Beijing, China[△]
 - 8 Humboldt University, D-10099 Berlin, FRG[§]
 - 9 University of Bologna and INFN-Sezione di Bologna, I-40126 Bologna, Italy
 - 10 Tata Institute of Fundamental Research, Bombay 400 005, India
 - 11 Northeastern University, Boston, MA 02115, USA
 - 12 Institute of Atomic Physics and University of Bucharest, R-76900 Bucharest, Romania
 - 13 Central Research Institute for Physics of the Hungarian Academy of Sciences, H-1525 Budapest 114, Hungary[‡]
 - 14 Massachusetts Institute of Technology, Cambridge, MA 02139, USA
 - 15 Lajos Kossuth University-ATOMKI, H-4010 Debrecen, Hungary[¶]
 - 16 INFN Sezione di Firenze and University of Florence, I-50125 Florence, Italy
 - 17 European Laboratory for Particle Physics, CERN, CH-1211 Geneva 23, Switzerland
 - 18 World Laboratory, FBLJA Project, CH-1211 Geneva 23, Switzerland
 - 19 University of Geneva, CH-1211 Geneva 4, Switzerland
 - 20 Chinese University of Science and Technology, USTC, Hefei, Anhui 230 029, China[△]
 - 21 SEFT, Research Institute for High Energy Physics, P.O. Box 9, SF-00014 Helsinki, Finland
 - 22 University of Lausanne, CH-1015 Lausanne, Switzerland
 - 23 INFN-Sezione di Lecce and Università Degli Studi di Lecce, I-73100 Lecce, Italy
 - 24 Institut de Physique Nucléaire de Lyon, IN2P3-CNRS, Université Claude Bernard, F-69622 Villeurbanne, France
 - 25 Centro de Investigaciones Energéticas, Medioambientales y Tecnológicas, CIEMAT, E-28040 Madrid, Spain^b
 - 26 INFN-Sezione di Milano, I-20133 Milan, Italy
 - 27 Institute of Theoretical and Experimental Physics, ITEP, Moscow, Russia
 - 28 INFN-Sezione di Napoli and University of Naples, I-80125 Naples, Italy
 - 29 Department of Natural Sciences, University of Cyprus, Nicosia, Cyprus
 - 30 University of Nijmegen and NIKHEF, NL-6525 ED Nijmegen, The Netherlands
 - 31 California Institute of Technology, Pasadena, CA 91125, USA
 - 32 INFN-Sezione di Perugia and Università Degli Studi di Perugia, I-06100 Perugia, Italy
 - 33 Carnegie Mellon University, Pittsburgh, PA 15213, USA
 - 34 Princeton University, Princeton, NJ 08544, USA
 - 35 INFN-Sezione di Roma and University of Rome, "La Sapienza", I-00185 Rome, Italy
 - 36 Nuclear Physics Institute, St. Petersburg, Russia
 - 37 University and INFN, Salerno, I-84100 Salerno, Italy
 - 38 University of California, San Diego, CA 92093, USA
 - 39 Dept. de Física de Partículas Elementales, Univ. de Santiago, E-15706 Santiago de Compostela, Spain
 - 40 Bulgarian Academy of Sciences, Central Lab. of Mechatronics and Instrumentation, BU-1113 Sofia, Bulgaria
 - 41 Center for High Energy Physics, Adv. Inst. of Sciences and Technology, 305-701 Taejeon, Republic of Korea
 - 42 University of Alabama, Tuscaloosa, AL 35486, USA
 - 43 Utrecht University and NIKHEF, NL-3584 CB Utrecht, The Netherlands
 - 44 Purdue University, West Lafayette, IN 47907, USA
 - 45 Paul Scherrer Institut, PSI, CH-5232 Villigen, Switzerland
 - 46 DESY, D-15738 Zeuthen, FRG
 - 47 Eidgenössische Technische Hochschule, ETH Zürich, CH-8093 Zürich, Switzerland
 - 48 University of Hamburg, D-22761 Hamburg, FRG
 - 49 National Central University, Chung-Li, Taiwan, China
 - 50 Department of Physics, National Tsing Hua University, Taiwan, China
- [§] Supported by the German Bundesministerium für Bildung, Wissenschaft, Forschung und Technologie
[‡] Supported by the Hungarian OTKA fund under contract numbers T019181, F023259 and T024011.
[¶] Also supported by the Hungarian OTKA fund under contract numbers T22238 and T026178.
^b Supported also by the Comisión Interministerial de Ciencia y Tecnología.
[‡] Also supported by CONICET and Universidad Nacional de La Plata, CC 67, 1900 La Plata, Argentina.
[◇] Also supported by Panjab University, Chandigarh-160014, India.
[△] Supported by the National Natural Science Foundation of China.
[†] Deceased.

Scalar electron selections					
ΔM (GeV)		3 – 5	10 – 40	60 – 90	
E_{lep} (GeV)	\leq	5.34	37.4	59.8	
ΣE_{lep} (GeV)	\geq	4.45	16.9	65.6	
E_{vis}/\sqrt{s}	\leq	0.12	0.36	0.63	
p_{\perp} (GeV)	\geq	3.62	1.45	8.95	
Acollinearity (rad)	\leq	2.26	3.10	–	
Acoplanarity (rad)	\leq	2.95	3.08	3.01	
E_{25}^{\perp} (GeV)	\leq	–	3.8	7.51	
E_{25} (GeV)	\leq	0.28	3.2	3.52	
E_{60}^b (GeV)	\leq	2.93	3.7	4.59	
$\sin(\theta_{miss})$	\geq	0.46	0.60	0.20	
E_{TTL} (GeV)	\geq	3.22	3.97	2.70	
Scalar muon selections					
ΔM (GeV)		3 – 5	10 – 40	60 – 90	
E_{lep} (GeV)	\leq	9.97	25.6	78.4	
E_{vis}/\sqrt{s}	\leq	0.16	0.30	0.58	
p_{\perp} (GeV)	\geq	2.69	8.53	11.2	
Acollinearity (rad)	\leq	3.09	3.09	2.41	
Acoplanarity (rad)	\leq	2.90	3.11	2.44	
E_{25}^{\perp} (GeV)	\leq	–	3.97	4.04	
E_{25} (GeV)	\leq	1.0	2.93	3.43	
E_{60}^b (GeV)	\leq	9.94	7.79	6.67	
$\sin(\theta_{miss})$	\geq	0.80	0.53	0.35	
E_{TTL} (GeV)	\geq	2.44	2.35	4.99	
Scalar tau selections					
ΔM (GeV)		3 – 7	7 – 15	15 – 30	30 – 90
E_{vis}/\sqrt{s}	\geq	0.04	0.06	0.08	0.11
E_{vis} (GeV)	\leq	21.9	38.1	54.4	76.1
p_{\perp} (GeV)	\geq	3.68	9.43	9.12	13.7
p_{\perp}/E_{vis}	\geq	0.08	0.36	0.19	0.30
Acollinearity (rad)	\leq	3.08	2.98	3.14	3.03
Acoplanarity (rad)	\leq	3.13	3.08	3.07	2.77
$\sin(\theta_{miss})$	\geq	0.85	0.67	0.58	0.55
E_{25}^{\perp} (GeV)	\leq	8.97	7.24	1.56	0.87
E_{TTJ} (GeV)	\geq	2.14	2.23	3.81	0.89
E_{TTJ}/p_{\perp}	\geq	0.21	0.13	0.13	0.04
Max track acoplanarity (rad)	\leq	2.98	2.97	2.93	2.66
y_{\perp}	\leq	0.38	0.33	0.36	0.73
E^{ℓ} (GeV)	\leq	14.3	33.8	50.8	62.2

Table 1: Optimised cut values for the scalar lepton searches for the different ΔM ranges. They are determined with the optimisation procedure described in Section 3.1.

	Low ΔM		Medium ΔM		High ΔM		Combined	
	N_{data}	N_{exp}	N_{data}	N_{exp}	N_{data}	N_{exp}	N_{data}	N_{exp}
\tilde{e}	7	6.0	3	4.8	11	12.4	21	23.0
$\tilde{\mu}$	10	11.5	2	1.0	8	9.1	19	21.0
$\tilde{\tau}$	23	23.1	5	7.5	33	29.4	56	51.6

Table 2: Results of the acoplanar lepton searches: N_{data} is the number of observed events and N_{exp} is the number of expected events from Standard Model processes for the total integrated luminosity collected at $\sqrt{s} = 189$ GeV.

$e^+e^- \rightarrow$	$\sqrt{s} = 189$ GeV					
	$M_{\tilde{e}^\pm} = 90$ GeV		$M_{\tilde{\mu}^\pm} = 80$ GeV		$M_{\tilde{\tau}^\pm} = 70$ GeV	
	$\tilde{e}^\pm\tilde{e}^\mp$		$\tilde{\mu}^\pm\tilde{\mu}^\mp$		$\tilde{\tau}^\pm\tilde{\tau}^\mp$	
$\Delta M(\text{GeV})$	ϵ (%)	N_{exp}	ϵ (%)	N_{exp}	ϵ (%)	N_{exp}
3	20.4	2.3	11.5	11.5	1.4	23.1
5	18.7	5.9	24.0	12.3	6.4	23.1
10	44.5	4.8	33.3	1.0	9.1	7.5
20	53.8	4.8	32.1	1.0	26.1	16.5
30	49.1	4.8	35.6	9.7	26.3	16.5
40	54.4	16.6	33.4	9.1	30.0	29.4
50	57.9	16.6	33.1	9.1	28.2	29.4
60	56.1	11.9	31.6	9.1	29.1	29.4
68	55.9	11.9	29.9	9.1	29.7	24.4
78	55.9	11.9	27.2	9.1	–	–
88	53.4	11.9	–	–	–	–

Table 3: Scalar electron, muon and tau efficiencies (ϵ) and number of events expected from Standard Model processes (N_{exp}). Results at $\sqrt{s} = 189$ GeV are listed as a function of ΔM for different $M_{\tilde{l}^\pm}$ values.

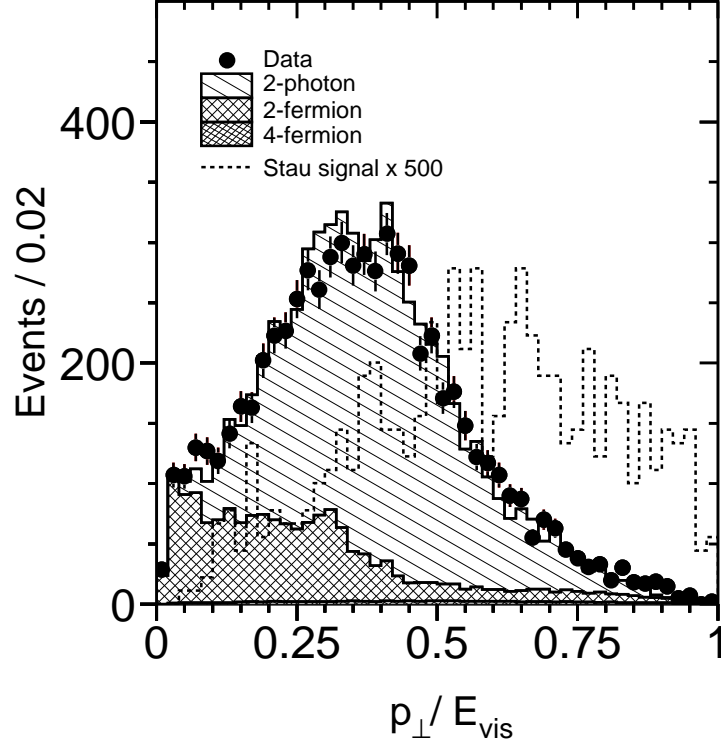


Figure 1: Normalised transverse momentum distributions p_{\perp}/E_{vis} for data and MC events at $\sqrt{s} = 189$ GeV after preselection. Contributions from 2-photon interactions, 2-fermion and 4-fermion final states are given separately. The distribution for an expected scalar tau signal with $M_{\tilde{\tau}_R} = 70$ GeV and $M_{\tilde{\chi}_1^0} = 55$ GeV is also shown.

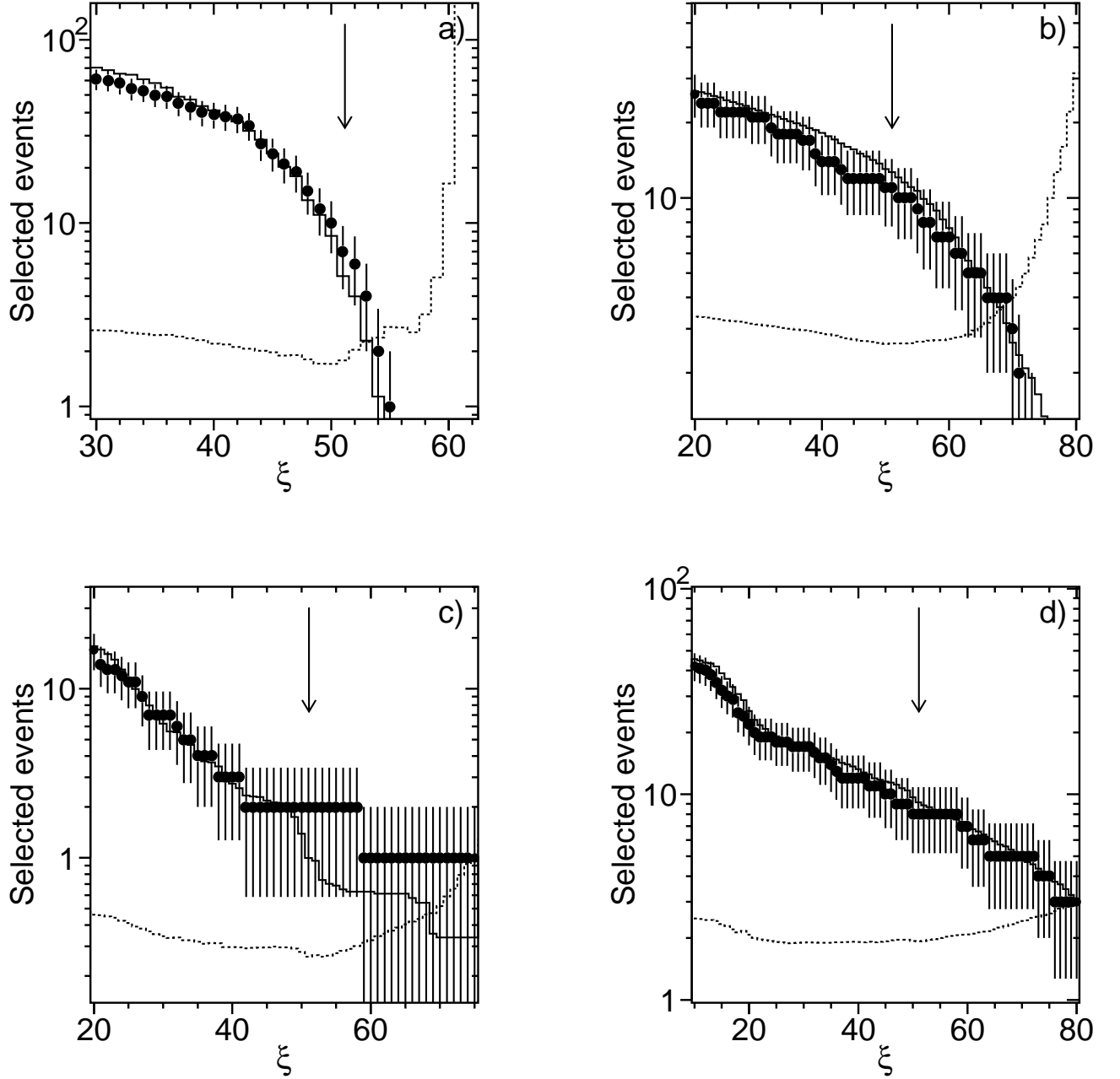


Figure 2: Number of events selected in data (dots), in Monte Carlo simulations of standard processes (solid line) and signal sensitivity (dashed line) as a function of selection cuts with increasing background rejection power. The vertical arrows show the ξ value corresponding to the optimised cuts. Distributions for the scalar electron low ΔM a) and high ΔM b), the scalar muon medium ΔM c) and high ΔM d) selections are shown.

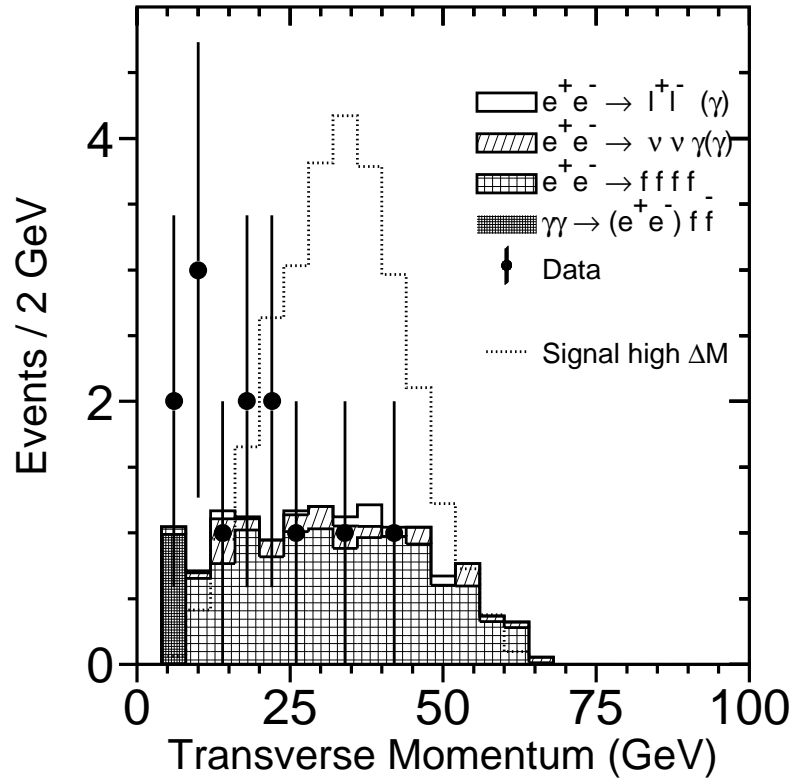


Figure 3: Transverse momentum distribution for the selected events in the single electron final state analysis. Data events observed at $\sqrt{s} = 189$ GeV are compared to Standard Model background processes and to the expected signal distributions with arbitrary normalisation.

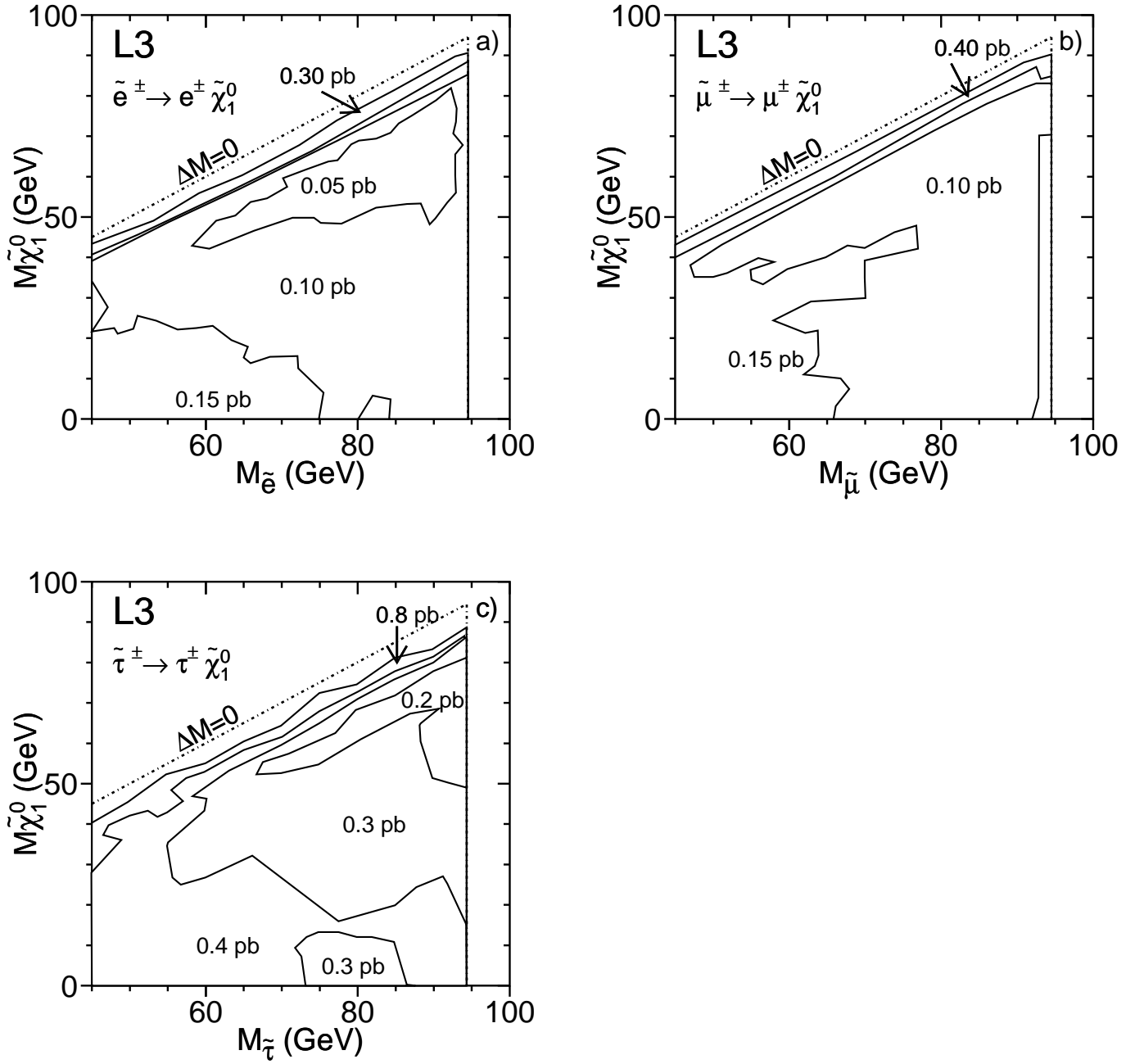


Figure 4: Upper limits on the production cross sections up to $\sqrt{s} = 189$ GeV shown in the mass plane $M_{\tilde{\ell}} - M_{\tilde{\chi}_1^0}$ for scalar leptons. Figures a), b) and c) show the limits for scalar electrons, muons and taus, respectively.

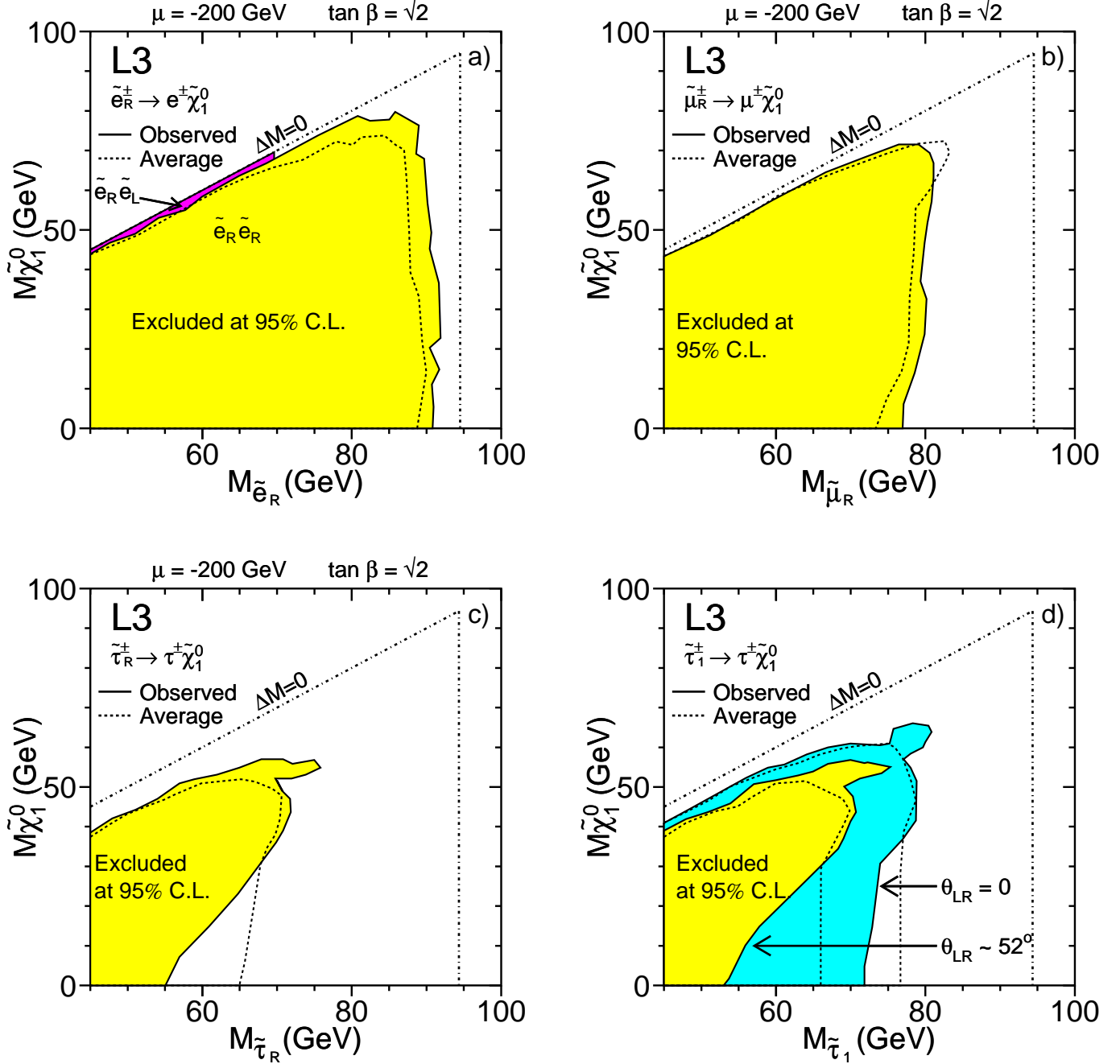


Figure 5: Mass limits on the scalar partners of right-handed electrons a), muons b) and taus c) as a function of the neutralino mass $M_{\tilde{\chi}_1^0}$. d) shows the exclusion for the scalar tau, when mixing between $\tilde{\tau}_R$ and $\tilde{\tau}_L$ occurs, for the minimal and maximal cross sections. These four figures are obtained using only the upper limits on the cross section from direct searches at centre-of-mass energies between 130 GeV and 189 GeV. The dashed lines show the average limits obtained with Monte Carlo trials with background only.

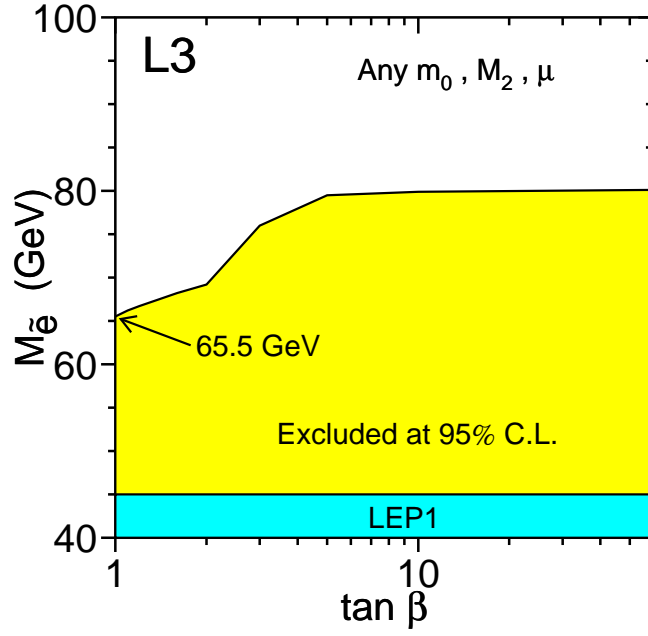


Figure 6: Lower limit on $M_{\tilde{e}_R}$ as a function of $\tan \beta$ and for any value of m_0 , M_2 , and μ . This limit is obtained with searches for acoplanar electrons at centre-of-mass energies between 130 GeV and 189 GeV, and single electrons at 189 GeV.

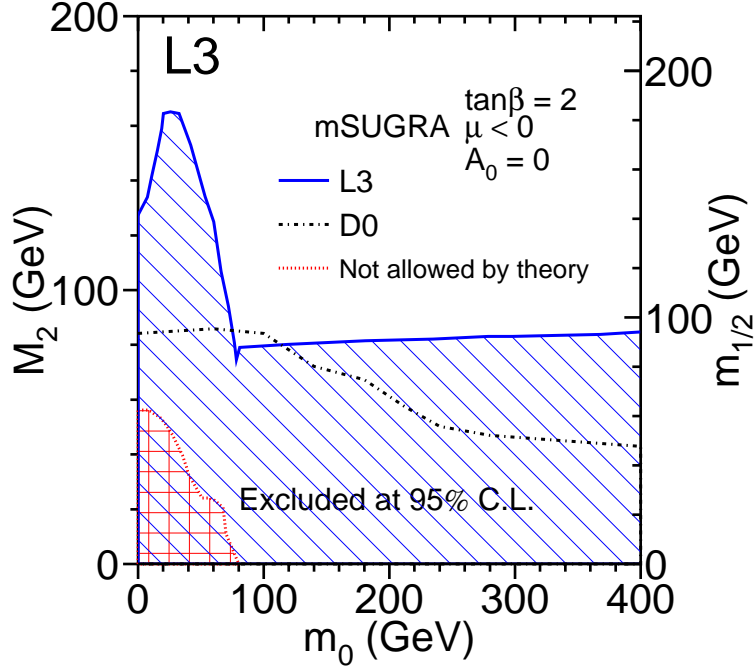


Figure 7: Exclusion domains in the $M_2 - m_0$ plane in the minimal SUGRA framework for $A_0 = 0$, $\tan \beta = 2$ and $\mu < 0$. The exclusions are obtained by combining scalar electron and muon searches with chargino and neutralino searches. The exclusion obtained by D0, at the Tevatron, from a search for gluinos and scalar quarks [24] is also shown. The small region in the bottom left corner is theoretically forbidden within mSUGRA.